ACAT2 contributes cholesteryl esters to newly secreted VLDL, whereas LCAT adds cholesteryl ester to LDL in mice

Richard G. Lee,* Ramesh Shah,* Janet K. Sawyer,* Robert L. Hamilton,† John S. Parks,* and Lawrence L. Rudel[1,*]

Arteriosclerosis Research Program,* Departments of Pathology and Biochemistry, Wake Forest University School of Medicine, Winston-Salem, NC; and Department of Anatomy,† University of California, San Francisco, San Francisco, CA

Abstract The relative contributions of ACAT2 and LCAT to the cholesteryl ester (CE) content of VLDL and LDL were measured. ACAT2 deficiency led to a significant decrease in the percentage of CE (37.2 ± 2.1% vs. 3.9 ± 0.8%) in plasma VLDL, with a concomitant increase in the percentage of triglyceride (33.0 ± 3.2% vs. 66.7 ± 2.5%). Interestingly, the absence of ACAT2 had no apparent effect on the percentage CE in LDL, whereas LCAT deficiency significantly decreased the CE percentage (38.6 ± 4.0% vs. 54.6 ± 1.9%) and significantly increased the phospholipid percentage (11.2 ± 0.9% vs. 19.3 ± 0.1%) of LDL. When both LCAT and ACAT2 were deficient, VLDL composition was similar to VLDL of the ACAT2-deficient mouse, whereas LDL was depleted in core lipids and enriched in surface lipids, appearing discoidal when observed by electron microscopy. We conclude that ACAT2 is important in the synthesis of VLDL CE, whereas LCAT is important in remodeling VLDL to LDL. Liver perfusions were performed, and perfusate apolipoprotein B accumulation rates in ACAT2-deficient mice were not significantly different from those of controls; perfusate VLDL CE decreased from 8.0 ± 0.8% in controls to 0 ± 0.7% in ACAT2-deficient mice. In conclusion, our data establish that ACAT2 provides core CE of newly secreted VLDL, whereas LCAT adds CE during LDL particle formation.— Lee, R. G., R. Shah, J. K. Sawyer, R. L. Hamilton, J. S. Parks, and L. L. Rudel. **ACAT2 contributes cholesteryl esters to newly secreted VLDL, whereas LCAT adds cholesteryl ester to LDL in mice. *J. Lipid Res.* 2005.** 46: **1205–1212.**

Supplementary key words acyl-CoA:cholesterol acyltransferase 2 • lecithin:cholesterol acyltransferase • low density lipoprotein • very low density lipoprotein • hepatocyte • apolipoprotein B

Abundant evidence in humans demonstrates that increased plasma concentrations of cholesterol in LDL and in VLDL are positively correlated with the development of atherosclerosis (1). A similar relationship between apolipoprotein B (apoB)-containing lipoprotein cholesterol and atherosclerosis has also been observed in studies carried out in LDL receptor-deficient ($LDLr^{-/-}$) mice (2). Typically, more than 70% of the cholesterol in LDL and VLDL is esterified. Therefore, the two enzymes responsible for the synthesis of plasma lipoprotein cholesteryl esters (CEs), LCAT and ACAT2, (3) are important determinants of both VLDL and LDL cholesterol concentrations and the subsequent development of atherosclerosis.

Several studies have provided evidence that the types of CEs that predominate in plasma contribute to the relative degree of atherogenicity (4). In humans, the percentage of cholesteryl linoleate was lower in coronary heart disease patients (5–8). The percentage of lipoprotein cholesteryl oleate and the rate of hepatic cholesteryl oleate secretion were positively related to the extent of atherosclerosis in monkeys (9, 10). A deficiency in plasma LCAT in mice resulted in higher percentages of saturated and monounsaturated CEs and more atherosclerosis (3, 11, 12). Therefore, polyunsaturated fatty acid containing CEs derived from LCAT are associated with decreased atherosclerosis (11), whereas saturated and monounsaturated CEs derived predominantly from ACAT2 (10) are associated with increased atherosclerosis.

The relative contribution of ACAT2 and LCAT to the CE pool in apoB lipoproteins is poorly understood. Humans and monkeys are species with plasma CETP, making it difficult to identify the relative contributions of ACAT2- and LCAT-derived CEs in individual lipoprotein classes. However, mice have no CETP, so the CEs in individual lipoprotein classes more likely represent the activity of the source enzyme, and it should be possible to monitor the relative amounts of CE from either enzyme actually secreted into plasma in VLDL versus incorporated into LDL during intravascular remodeling of VLDL into LDL. Furthermore, with the availability of mice with gene deletions of either ACAT2 or LCAT, the modifications of CE transport can be further identified.

Manuscript received 14 January 2005 and in revised form 1 March 2005.

Published, JLR Papers in Press, April 1, 2005.
DOI 10.1194/jlr.M500018-JLR200

[1] To whom correspondence should be addressed.
e-mail: lrudel@wfubmc.edu

This paper presents a novel approach to defining the contributions of LCAT and ACAT2 to the CEs within plasma VLDL and LDL. We used mice with targeted gene deletions of ACAT2 and LCAT to help define the contributions of each enzyme in LDLr$^{-/-}$ mice that maintain significant plasma LDL cholesterol concentrations. We also used isolated liver perfusion to uniquely define the role of ACAT2 in the production of liver-secreted VLDL CEs. Our results delineate distinct roles for hepatic ACAT2 and plasma LCAT in the production of plasma VLDL and LDL CE pools.

MATERIALS AND METHODS

Mice and diets

All mice used in these studies were housed at the Wake Forest University Medical School American Association for Accreditation of Laboratory Animal Care-approved animal facility, and the Institutional Animal Care and Use Committee approved all animal protocols. For the determination of apoB secretion rates, female *LDLr*$^{-/-}$ and *ACAT2*$^{-/-}$ *LDLr*$^{-/-}$ mice 4–10 months of age were used. Each animal was fed for a minimum of 4 weeks 10 g/day of a semisynthetic diet that contained palm oil as fat (10% of energy) and either a low cholesterol (0.02%, w/w) or a moderate cholesterol (0.18%, w/w) content. Complete diet compositions were described previously (13). For determination of the chemical composition of perfusate VLDL and plasma VLDL and LDL, male *LDLr*$^{-/-}$, *ACAT2*$^{-/-}$ *LDLr*$^{-/-}$, *LCAT*$^{-/-}$ *LDLr*$^{-/-}$, and *ACAT2*$^{-/-}$ *LCAT*$^{-/-}$ *LDLr*$^{-/-}$ mice were studied. All mice were mixtures of C57Bl/6 and SV129 backgrounds, with C57Bl/6 representing ~75% in all cases.

Preparation for liver perfusion

One day before perfusion, medium was made up as described previously (14). The perfusate consisted of Krebs-Ringer bicarbonate buffer containing essential and nonessential amino acids, glucose, penicillin, streptomycin, insulin, and hydrocortisone. Medium was continuously gassed with 95% O_2 and 5% CO_2 to maintain pH 7.4. Mice were exsanguinated via heart puncture, and erythrocytes were collected after centrifugation of the blood at 1,100 *g* for 20 min at 4°C. The red blood cells were then washed twice with 0.9% NaCl (w/v) and 0.01% (w/v) D-glucose to remove white blood cells and twice with perfusion media to remove saline and D-glucose. The washed erythrocytes were added to the perfusate medium to reach a final hematocrit of 10%.

Liver perfusion

The mouse was anesthetized by intramuscular injection of 2.5 mg of ketamine hydrochloride and 0.5 mg of xylazine. The animal was then weighed, and the abdomen was shaved in preparation for surgery. The animal was placed on its back on a flat surface maintained at 37°C. The abdomen was centered on the stage of a dissecting microscope, and a midline incision was made to expose the liver. The intestines were retracted to expose the portal vein, and two 6.0 sutures were then looped around the portal vein. The portal vein was cannulated with a 22 gauge BD Insyte Autoguard shielded intravenous catheter (Becton Dickinson), and the cannula was then secured to the portal vein with the two 6.0 sutures. The liver was immediately flushed with oxygenated perfusate medium (without red cells) at 1.0 ml/min using a peristaltic roller pump (Masterflex model 7565-10; Cole-Parmer Instrument Co., Chicago IL) with pump head (model 7017). Clearance of blood from the liver signified successful cannulation of the portal vein. The thorax was then opened, and two 6.0 sutures were looped around the vena cava. A 22 gauge shielded intravenous catheter (Becton Dickinson) was then inserted through the atrium of the heart into the vena cava, where it was secured using the two 6.0 sutures.

The mouse was then suspended on a nylon screen in a closed, humidified Plexiglas chamber maintained at a constant 37°C using a heat lamp controlled by a temperature regulator (Yellow Springs Instrument Co., Yellow Springs, OH). The entire perfusion system contained a total volume of 10 ml. Perfusate was continuously oxygenated with 95% O_2 and 5% CO_2 by passage through a Silastic tubing lung, and temperature was maintained at 37°C with a heat exchanger. Any macro emboli were removed using an inline 25 mm filter screen, whereas an inline bubble trap was positioned immediately before the portal vein cannula.

To begin the procedure, the liver was flushed of trapped plasma lipoproteins by recirculating medium containing erythrocytes for 30 min. At the end of this period, perfusate was exchanged with 10 ml of fresh medium containing erythrocytes and then continuously recirculated through the liver at the rate of 1 ml/min for 3 h. During the 3 h of perfusion, a 1.5 ml aliquot was removed every 30 min, and 1.5 ml of fresh medium containing erythrocytes was added back to the reservoir. At the end of the 3 h period, all 10 ml of perfusate was collected. The final perfusate and all time point samples were centrifuged at 4°C to separate the medium from the erythrocytes.

The quality of the experiment was monitored during perfusion by the outward appearance of the liver and the changing of perfusate from red to blue as it passed through the liver, indicating good oxygen use. In addition, the linearity of the total cholesterol and triglyceride (TG) accumulation rates throughout perfusion was also indicative of liver health.

Secretion rates of all lipoprotein lipid classes, including total cholesterol, free cholesterol (FC), TG, and phospholipid (PL), were determined with enzymatic assays to measure the amount of lipid in each time point sample. For assay, the lipids from each aliquot of perfusate were extracted by the Bligh-Dyer method (15), solubilized in 0.1% Triton X-100, and enzymatically quantified as described previously (16).

Quantitation of apoB

Lipoproteins were isolated from 0.5 ml aliquots of the 30, 60, 90, 120, 150, and 180 min liver perfusion samples by adjusting the density of each aliquot to 1.225 g/ml with KBr. The aliquot was centrifuged at 100, 000 *g* for 12 h in a TLA 100.2 rotor in an Optima™ MAX-E ultracentrifuge (Beckman), and the floated lipoproteins were harvested using a tube slicer. ApoB-100 and apoB-48 standards were made using sequential ultracentrifugation to isolate LDL in the $1.019 < d < 1.063$ g/ml range from plasma of apoB-100-only and apoB-48-only mice, respectively. Lipoprotein samples isolated from time points and standards were prepared by first adding 5.0 μg of BSA to each sample. TCA precipitation was then carried out by adding an equal volume of 20% TCA to each sample. The samples were chilled on ice and centrifuged, the supernatant was decanted, and the pellets were washed with 5% TCA to remove residual KBr. Delipidation of the samples was carried out by adding 1:1 ethanol/ethyl ether, and the protein was repelleted by centrifugation. The supernatant was decanted, and the washed, delipidated protein pellets were air-dried. Protein solubilization buffer [120 mM Tris, pH 6.8, 20% (v/v) glycerol, 4% (w/v) SDS, 0.1 M dithiothreitol, and 0.01% bromphenol blue] was added, and each sample was heated at 50°C for 1 h with mixing to ensure solubilization of the protein. The samples were then boiled for 5 min, and samples and standards were loaded onto a 4–20% polyacrylamide gradient gel containing SDS. Electrophoresis was carried out for 6 h at 40 V, and

TABLE 1. Accumulation rates of lipid during 3 h of liver perfusion of knockout mice fed a 0.02% cholesterol diet

Genotype	Lipid Accumulation			
	FC	CE	TG	PL
	μg/min/g liver			
LDLr$^{-/-}$ (n = 3)	1.6 (0.2)^{a}	1.9 (0.6)^{a}	11.4 (3.7)^{a,b}	6.6 (1.3)^{a}
ACAT2$^{-/-}$ *LDLr*$^{-/-}$ (n = 3)	1.3 (0.03)^{a,b}	0.3 (.08)^{b,c}	16.2 (3.0)^{b}	4.0 (0.6)^{b}
LCAT$^{-/-}$ *LDLr*$^{-/-}$ (n = 3)	1.2 (0.07)^{b}	1.0 (0.2)^{a,c}	5.8 (1.3)^{a}	2.7 (0.2)^{b}
ACAT2$^{-/-}$ *LCAT*$^{-/-}$ *LDLr*$^{-/-}$ (n = 4)	1.2 (0.1)^{a,b}	0.02 (.01)^{b}	10.2 (0.7)^{a,b}	3.5 (0.4)^{b}

CE, cholesteryl ester; FC, free cholesterol; LDLr$^{-/-}$, LDL receptor-deficient; PL, phospholipid; TG, triglyceride. Lipid contents of 30 min time points were quantified as described in Materials and Methods, and resulting values were used to calculate lipid accumulation rates. Values represent means and (SEM). Statistically significant differences were determined by ANOVA and Fisher's post hoc test. Values in the same column with different letters are significantly different ($P < 0.05$); values with the same letters are not different from each other.

the gel was then blotted onto nitrocellulose for 2 h at 100 V. The blot was blocked in 3% nonfat dry milk in TBST (150 mM NaCl, 20 mM Tris, pH 7.4, and 0.05% Tween 20) for 1 h and then incubated for 2 h at room temperature in a rabbit anti-mouse apoB polyclonal antibody (Bio-Rad) diluted 1:5,000 in primary antibody buffer (TBST with 0.5 mg/ml $MgCl_2$). The blot was washed and incubated in a 1:15,000 dilution of a goat anti-rabbit horseradish peroxidase-conjugated secondary antibody (Sigma) for 1 h. The blot was developed using ECL SuperSignal reagent (Pierce), and apoB-100 and apoB-48 protein mass were quantified using the Chemi Imager 5500 (Alpha Innotech).

Chemical and morphologic analysis of VLDL and LDL composition

For the isolation of VLDL from plasma and perfusate, samples were centrifuged at 100,000 rpm for 90 min at 15°C in a Beckman TLA 100.2 rotor at a density of 1.006 g/ml, and the floated lipoproteins were collected from the top of the tube using a tube slicer. For collection of LDL from plasma, the bottom fraction of the 1.006 g/ml spin was adjusted to a density of 1.019 g/ml with KBr and centrifuged at 100,000 rpm for 4.5 h at 15°C, and the intermediate density lipoprotein was collected from the top of the tube using a tube slicer. The bottom fraction of the intermediate density lipoprotein spin was adjusted to a density of 1.080 g/ml and centrifuged at 100,000 rpm for 12 h at 15°C, and the LDL was collected from the top of the tube using a tube slicer.

Chemical compositions and plasma concentrations of lipoproteins were determined with enzymatic assays for TG, FC, and total cholesterol (FC by Wako Chemicals USA, total cholesterol and TG by Roche Diagnostics) using the protocols provided by the manufacturer. CE mass was calculated by subtracting FC from total cholesterol and multiplying the result by 1.67 to include the mass of the fatty acyl chain. Phospholipid was quantified by either enzymatic analysis (Wako Chemicals USA) of phosphatidylcholine using the manufacturer's protocol or, occasionally, by measuring inorganic phosphorus by the method of Fiske and Subba-Row (17). Protein was determined by the method of Lowry et al. (18). For chemical compositions, the masses for individual constituents were summed, and the data are expressed as percentage of total lipoprotein weight. Plasma lipid concentrations were calculated by dividing the total mass of FC, CE, TG, or PL in the VLDL or LDL fraction by the initial volume of the plasma sample.

Negative stain electron microscopy was carried out as described previously (19). Perfusate VLDL and plasma VLDL and LDL were isolated as described above; LDL was dialyzed against saline to remove KBr. Protein concentration was then adjusted to 1 mg/ml, and negative stain electron microscopy was carried out with 2% potassium phosphotungstate on formvar, carbon-coated 200 mesh copper grids.

Statistical analyses

Data were evaluated using one-way ANOVA for genotype with post hoc analyses by Fisher's protected least significant difference test. Statistical significance was considered at $P < 0.05$. The outcomes for post hoc analyses are as indicated.

RESULTS

In the first set of experiments, the effect of ACAT2 and/or LCAT deficiency on perfusate lipid accumulation rates was examined in livers of animals fed a low-cholesterol diet (**Table 1**). In the liver perfusate of *ACAT2*$^{-/-}$ *LDLr*$^{-/-}$ compared with *LDLr*$^{-/-}$ mice, the primary difference was the 87% decrease in CE accumulation rate; other lipid secretion rates were not significantly different. CE accumulation rates were also low in the *ACAT2*$^{-/-}$ *LCAT*$^{-/-}$ *LDLr*$^{-/-}$ mouse livers, but this rate was not different from that of the *ACAT2*$^{-/-}$ *LDLr*$^{-/-}$ mice. These data suggest that almost all perfusate CE is derived from ACAT2 and is therefore missing when ACAT2 is deficient. Only ~15% of the perfusate CE appears to be derived from LCAT. A slight decrease in perfusate FC was also seen in the *LCAT*$^{-/-}$ *LDLr*$^{-/-}$ mice, a finding opposite to what might have been expected. TG accumulation rates were generally comparable among groups, although curiously, a higher value was found for the *ACAT2*$^{-/-}$ *LDLr*$^{-/-}$ mice compared with the *LCAT*$^{-/-}$ *LDLr*$^{-/-}$ mice. The PL accumulation rate in the

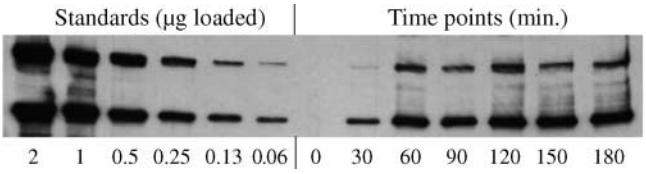

Fig. 1. Representative quantitative apolipoprotein B (apoB) Western blot of liver perfusate from an ACAT2-deficient/LDL receptor-deficient (*ACAT2*$^{-/-}$ *LDLr*$^{-/-}$) mouse fed a 0.02% cholesterol diet. Standards and time points were prepared and immunoblotted using a polyclonal antibody raised against mouse apoB-100 as described in Materials and Methods. Lanes 1–6 represent serial dilutions of standards, with amounts of either apoB-100 or apoB-48 indicated at bottom. Lanes 7–13 represent time points from 3 h liver perfusion, with the time points indicated at bottom.

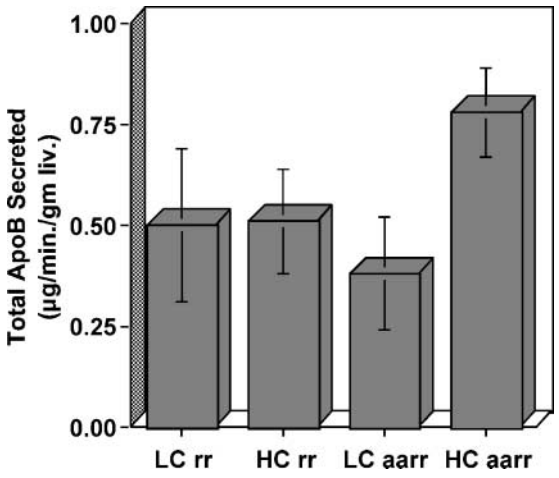

Fig. 2. ApoB accumulation rates in liver perfusate of *ACAT2*$^{-/-}$ *LDLr*$^{-/-}$ (aarr) and *LDLr*$^{-/-}$ (rr) mice fed either a high-cholesterol (HC) or a low-cholesterol (LC) diet. ApoB-100 and apoB-48 bands from immunoblots were quantified as described in Materials and Methods, and accumulation rates were calculated. Values represent mean total apoB (apoB-100 plus apoB-48) accumulation rates ± SEM. n = 4 for all groups except the low-cholesterol *LDLr*$^{-/-}$ mice, which had n = 3.

LDLr$^{-/-}$ control mice was significantly higher compared with those of the other three genotypes. Although these data demonstrated that ACAT2 is necessary for the hepatic secretion of CE, it was not required for significant amounts of the other lipoprotein lipids. We hypothesized that the ACAT2-related depletion in CE accumulation in the perfusate was not attributable to a decrease in the secretion of apoB into the perfusate.

We analyzed the effect of ACAT2 deficiency on apoB-48 and apoB-100 accumulation rates during liver perfusion in *LDLr*$^{-/-}$ and *ACAT2*$^{-/-}$ *LDLr*$^{-/-}$ mice fed two different levels of dietary cholesterol. The data shown in **Fig. 1** illustrate a complete data set for one animal and also show a standard curve for both apoB-48 and apoB-100. Despite equivalent amounts of apoB-48 and apoB-100 standards being loaded on the gel, the apoB-100 bands on the immunoblot were consistently less intense than the corresponding apoB-48 band, a result likely attributable to the less efficient transfer of the larger apoB-100 protein from the gel to the nitrocellulose during Western blotting. Importantly, estimates of appearance rates of either form of apoB were made from the appropriate standard curve. The data in **Fig. 2** show the averaged data for all 15 animals studied. The total apoB accumulation rate of the *ACAT2*$^{-/-}$ *LDLr*$^{-/-}$ mice was no different from that of the *LDLr*$^{-/-}$ controls. Similarly, the accumulation rate of apoB in the perfusate of either genotype was not different when the animals were fed cholesterol-enriched diets (Fig. 2). The apoB-48/apoB-100 ratio averaged ~1 for each group and did not vary by genotype or dietary cholesterol level.

More than 90% of the cholesterol and 99% of the TG were located in the VLDL (d < 1.006 g/ml) fraction of the liver perfusate lipoproteins initially floated at d < 1.225 g/ml (data not shown); therefore, we limited our analysis of perfusate lipoproteins to the VLDL fraction. Perfusate VLDLs isolated by ultracentrifugation at a density of 1.006 g/ml were analyzed for FC, CE, TG, PL, and protein content. Values are expressed as the percentage contribution to the total VLDL mass (**Table 2**). As expected, perfusate VLDL from mice lacking ACAT2 had a decreased percentage CE mass (0 ± 0.7% and 1 ± 0.4% in *ACAT2*$^{-/-}$ *LDLr*$^{-/-}$ and *ACAT2*$^{-/-}$ *LCAT*$^{-/-}$ *LDLr*$^{-/-}$ mice, respectively) compared with VLDL from *LDLr*$^{-/-}$ mice (8.0 ± 0.8%). The tendency for VLDL percentage TG mass to be greater in *ACAT2*$^{-/-}$ *LDLr*$^{-/-}$ and *ACAT2*$^{-/-}$ *LCAT*$^{-/-}$ *LDLr*$^{-/-}$ mice reached statistical significance compared with VLDL TG in *LCAT*$^{-/-}$ *LDLr*$^{-/-}$ mice but not compared with that for *LDLr*$^{-/-}$ mice. There were no significant differences in the percentage surface lipids (FC and PL) and protein among the four genotypes.

Plasma VLDL and LDL lipid concentrations were also determined (**Fig. 3**). In *ACAT2*$^{-/-}$ *LDLr*$^{-/-}$, *LCAT*$^{-/-}$ *LDLr*$^{-/-}$, and *ACAT2*$^{-/-}$ *LCAT*$^{-/-}$ *LDLr*$^{-/-}$ mice, VLDL CE concentrations were significantly decreased compared with those of *LDLr*$^{-/-}$ mice (Fig. 3A). Furthermore, mice lacking ACAT2 had significantly lower VLDL CE concentrations compared with *LCAT*$^{-/-}$ *LDLr*$^{-/-}$ mice. VLDL TG concentrations were similar among all genotypes. VLDL FC concentrations were significantly decreased in the *ACAT2*$^{-/-}$ *LCAT*$^{-/-}$ *LDLr*$^{-/-}$ mice compared with *LDLr*$^{-/-}$ mice, whereas VLDL PL concentrations were similar among all genotypes (Fig. 3B). *LCAT*$^{-/-}$ *LDLr*$^{-/-}$ and *ACAT2*$^{-/-}$ *LCAT*$^{-/-}$ *LDLr*$^{-/-}$ mice had significantly lower LDL CE concentrations compared with *LDLr*$^{-/-}$ mice (Fig. 3C). Unexpectedly, *ACAT2*$^{-/-}$ *LDLr*$^{-/-}$ mice had significantly higher LDL CE concentrations compared with the other three genotypes. LDL TG concentrations were similar in all four genotypes. *ACAT2*$^{-/-}$

TABLE 2. Composition of knockout mouse VLDL (d < 1.006) isolated from perfusate after 3 h of liver perfusion

	Percentage of Total VLDL Mass				
Genotype	FC	CE	TG	PL	Protein
LDLr$^{-/-}$ (n = 3)	5.9 (0.4)	8.0 (0.8)^{a}	62.3 (1.9)^{a,b}	15.0 (0.7)	8.9 (0.8)
ACAT2$^{-/-}$ *LDLr*$^{-/-}$ (n = 4)	7.0 (0.6)	0 (0.7)^{b}	70.7 (1.8)^{b}	13.7 (0.8)	9.6 (0.6)
LCAT$^{-/-}$ *LDLr*$^{-/-}$ (n = 3)	8.0 (0.7)	9.6 (2.0)^{a}	57.6 (4.1)^{a}	15.0 (1.4)	9.7 (0.8)
ACAT2$^{-/-}$ *LCAT*$^{-/-}$ *LDLr*$^{-/-}$ (n = 4)	6.0 (0.7)	1.0 (0.4)^{b}	71.9 (4.2)^{b}	12.5 (1.5)	8.5 (1.8)

VLDL isolation and lipid and protein content were quantified as described in Materials and Methods. Values were calculated as percentages of the total mass of the VLDL lipoprotein. Values represent means and (SEM). Statistical significance is indicated as described for Table 1, and values with different letters in the same column are statistically different ($P < 0.05$). Columns with no letters indicate no significant differences ($P > 0.05$).

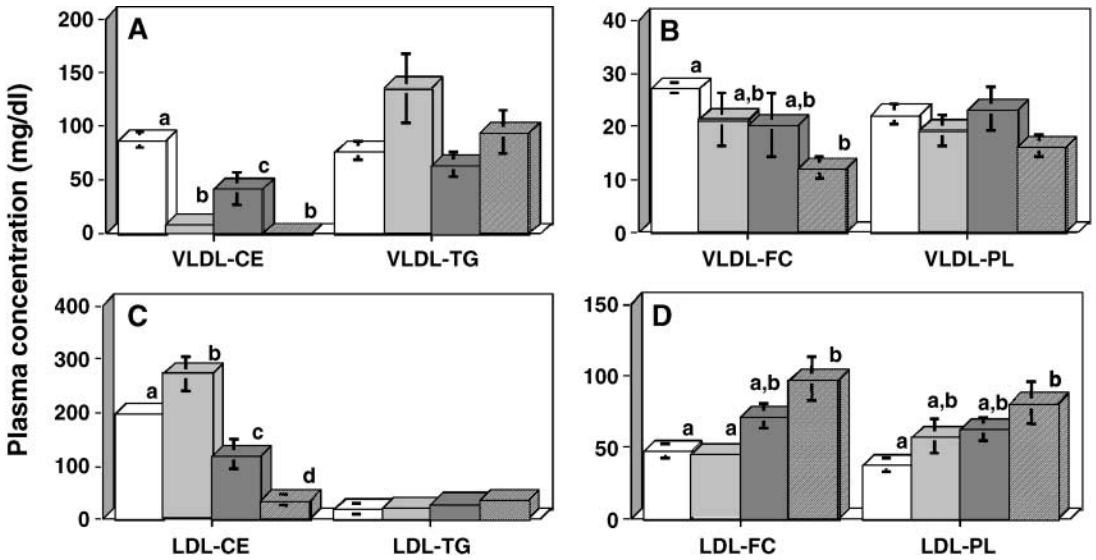

Fig. 3. VLDL and LDL plasma lipid concentrations in knockout mice fed a 0.02% cholesterol diet. Plasma from *LDLr*$^{-/-}$ (white bars; n = 3), *ACAT2*$^{-/-}$ *LDLr*$^{-/-}$ (light gray bars; n = 5), *LCAT*$^{-/-}$ *LDLr*$^{-/-}$ (dark gray bars; n = 3), and *ACAT2*$^{-/-}$ *LCAT*$^{-/-}$ *LDLr*$^{-/-}$ (hatched bars; n = 6) mice underwent sequential ultracentrifugation, and lipid concentrations were determined as described in Materials and Methods. A: VLDL cholesteryl ester (CE) and triglyceride (TG) plasma concentrations in knockout mice. B: VLDL free cholesterol (FC) and phospholipid (PL) plasma concentrations in knockout mice. C: LDL CE and TG plasma concentrations in knockout mice. D: LDL FC and PL plasma concentrations in knockout mice. For each lipoprotein lipid comparison, different letters denote significantly different ($P < 0.05$) values among genotypes. Error bars represent mean ± SEM.

LCAT$^{-/-}$ *LDLr*$^{-/-}$ mice had significantly increased LDL FC and PL values compared with *LDLr*$^{-/-}$ mice (Fig. 3D).

To determine the relationship between the chemical composition of VLDL secreted from liver and the chemical composition of the VLDL and LDL circulating in plasma, blood plasma VLDL and LDL from each of the mouse lines were isolated by sequential ultracentrifugation. Similar to the outcome for perfusate VLDL, the percentage of surface constituents of plasma VLDL among the four genotypes were not significantly different (**Table 3**), although the *LCAT*$^{-/-}$ *LDLr*$^{-/-}$ mice tended to have slightly higher percentages for surface phospholipids and protein and an apparently higher average surface-to-core ratio (**Table 4**).

Comparison of the VLDL surface lipids in plasma (Table 3) versus perfusate (Table 2) indicated that percentage FC was lower in the perfusate compared with the plasma VLDL, whereas percentage PL was somewhat higher in the perfusate than in the plasma, at least for the *LDLr*$^{-/-}$ and *ACAT2*$^{-/-}$ *LDLr*$^{-/-}$ mice. In the *LDLr*$^{-/-}$ mice, percentage CE mass in the VLDL increased from 8.0 ± 0.8% in the perfusate to 37.2 ± 2.1% in the plasma VLDL. In *LCAT*$^{-/-}$ *LDLr*$^{-/-}$ mice, it increased from 9.6 ± 2.0% to 23.6 ± 3.7%. Just as in the perfusate, percentage CE mass in the plasma VLDL of *ACAT2*$^{-/-}$ mice was significantly depleted to 3.9 ± 0.8% and 0 ± 0.9% for *ACAT2*$^{-/-}$ *LDLr*$^{-/-}$ and *ACAT2*$^{-/-}$ *LCAT*$^{-/-}$ *LDLr*$^{-/-}$ mice, respectively. However, these differences in CE did not result in significant differences between the ratio of surface to core constituents of the plasma versus the perfusate VLDL (Table 4), because, at the same time as the depletion of CE in the core occurred, the percentage TG mass in the plasma VLDL was increased significantly (66.7 ± 2.5% and 68.3 ± 3.3%). How core lipid composition was adjusted in the absence of plasma CETP is uncertain, but it is clear that for plasma VLDL, similar to the results for VLDL of liver perfusate, ACAT2 deficiency led to the depletion of CE in the core of the VLDL; compensation with TG occurred in both strains of *ACAT2*$^{-/-}$ mice (i.e., *ACAT2*$^{-/-}$ LDLr$^{-/-}$ and *ACAT2*$^{-/-}$ *LCAT*$^{-/-}$ *LDLr*$^{-/-}$ animals).

The chemical compositions of LDL isolated from plasma

TABLE 3. Composition of VLDL (d < 1.006) isolated from plasma of knockout mice fed a 0.02% cholesterol diet

	Percentage of Total VLDL Mass				
Genotype	FC	CE	TG	PL	Protein
LDLr$^{-/-}$ (n = 3)	11.5 (0.2)	37.2 (2.1)^{a}	33.0 (3.2)^{a}	9.5 (0.9)	8.8 (1.7)
ACAT2$^{-/-}$ *LDLr*$^{-/-}$ (n = 5)	10.6 (0.5)	3.9 (0.8)^{b}	66.7 (2.5)^{b}	10.2 (1.4)	8.6 (1.0)
LCAT$^{-/-}$ *LDLr*$^{-/-}$ (n = 3)	12.1 (1.0)	23.6 (3.7)^{c}	40.1 (3.9)^{a}	14.7 (2.1)	9.6 (0.7)
ACAT2$^{-/-}$ *LCAT*$^{-/-}$ *LDLR*$^{-/-}$ (n = 6)	10.2 (0.8)	0 (0.9)^{d}	68.3 (3.3)^{b}	13.6 (2.2)	10.3 (1.4)

VLDL isolation and lipid and protein content were quantified as described in Materials and Methods. Values were calculated as percentages of the total mass of the VLDL lipoprotein. Values represent means and (SEM). Values in the same column with different letters denote statistically significant differences ($P < 0.05$); columns with no letters indicate no significant differences ($P > 0.05$).

TABLE 4. Surface-to-core ratios of VLDL isolated from perfusate or plasma and LDL isolated from plasma

Genotype	Surface Components-Core Components		
	Perfusate VLDL	Plasma VLDL	Plasma LDL
LDLr$^{-/-}$	0.43 (0.03)	0.43 (0.05)	0.68 (0.02)
ACAT2$^{-/-}$ *LDLr*$^{-/-}$	0.44 (0.03)	0.43 (0.06)	0.79 (0.07)
LCAT$^{-/-}$ *LDLr*$^{-/-}$	0.49 (0.06)	0.58 (0.06)	1.13 (0.18)
ACAT2$^{-/-}$ *LCAT*$^{-/-}$ *LDLr*$^{-/-}$	0.39 (0.08)	0.56 (0.13)	7.22 (1.16)[a]

Values were calculated by dividing the sum of the percentage of the total mass of the lipoprotein that resided on the surface (FC, PL, and protein) by the sum of the percentage of the total mass that was contained in the core (CE and TG). Values represent means and (SEM).

[a] Statistically significant difference ($P < 0.05$) compared with *LDLr*$^{-/-}$ controls in the same column.

of the mice were also analyzed (**Table 5**). No CEs were present in the LDL of mice without both ACAT2 and LCAT. The percentage of CE in *LCAT2*$^{-/-}$ *LDLr*$^{-/-}$ mice was significantly lower than in the *LDLr*$^{-/-}$ control mice, whereas in *ACAT2*$^{-/-}$ *LDLr*$^{-/-}$ mice, the percentage CE mass in the LDL was not significantly different from that in *LDLr*$^{-/-}$ mice. LCAT is apparently able to synthesize LDL CE and compensate for the loss of ACAT2-derived CE in *ACAT2*$^{-/-}$ *LDLr*$^{-/-}$ mice. Unlike the perfusate and plasma VLDL, there were differences in the percentage of total mass on the surface for LDL of the different genotypes, with plasma LDL of the *LCAT*$^{-/-}$ mice having higher FC and PL percentages. In the *ACAT2*$^{-/-}$ *LCAT*$^{-/-}$ *LDLr*$^{-/-}$ mice, 88% of the total LDL mass was on the surface FC, PL, and protein (Table 5). Interestingly, the percentages of LDL CE in the *ACAT2*$^{-/-}$ *LDLr*$^{-/-}$ mice versus the *LCAT*$^{-/-}$ *LDLr*$^{-/-}$ mice suggest that a partial compensation occurs in the absence of either enzyme such that LDL contains more CE than was contributed to LDL by that enzyme in mice with both enzymes being functional.

Given the differences in chemical composition, we examined the morphology of perfusate VLDL and plasma VLDL and LDL of *ACAT2*$^{-/-}$ *LDLr*$^{-/-}$ mice (**Fig. 4A**, **C**, **E**) and *ACAT2*$^{-/-}$ *LCAT*$^{-/-}$ *LDLr*$^{-/-}$ mice (Fig. 4B, D, E) by negative stain electron microscopy. For both perfusate and plasma VLDL, there were few apparent morphologic differences between the two genotypes. The presence of an abundance of very small, apparently spherical particles in the plasma VLDL of the *ACAT2*$^{-/-}$ *LCAT*$^{-/-}$ *LDLr*$^{-/-}$ mice was not as apparent in the plasma VLDL of the *ACAT2*$^{-/-}$ *LDLr*$^{-/-}$ mice. These particles floated at d < 1.006 g/ml yet were smaller than LDL; some of these particles were present in perfusate VLDL, but their significance remains unknown. Analysis of LDL showed that lipoproteins in the *ACAT2*$^{-/-}$ *LDLr*$^{-/-}$ mice were spherical, whereas the LDL of the *ACAT2*$^{-/-}$ *LCAT*$^{-/-}$ *LDLr*$^{-/-}$ mice had a heterogeneous appearance, with a smaller percentage being spherical. A large percentage had a flattened appearance. The enrichment of surface lipids and depletion of core lipids in the *ACAT2*$^{-/-}$ *LCAT*$^{-/-}$ *LDLr*$^{-/-}$ mice led the lipoproteins to take on a flattened, discoidal appearance; these are likely surface lipid-rich remnants that are seen only in LCAT deficiency. These structures are not seen in LDL of *ACAT2*$^{-/-}$ mice.

DISCUSSION

The purpose of this study was *1*) to determine whether ACAT2 deficiency decreased apoB secretion rates during mouse liver perfusion by decreasing CE substrate, and *2*) to determine the effects of ACAT2 and/or LCAT deficiency on the chemical composition of apoB-containing lipoproteins isolated from liver perfusion or plasma. Results from our experiments indicate that ACAT2 deficiency did not decrease the number of VLDL particles secreted but did deplete CE in the core of the VLDL isolated from perfusate and plasma, leading to a significant decrease in the concentration of plasma VLDL CE. Although ACAT2 deficiency had an effect on the core composition of VLDL, there were no significant effects on the percentage of CE in the core of the LDL, presumably because of the ability of LCAT to compensate by esterifying cholesterol on LDL, which caused LDL CE concentrations to be increased significantly in *ACAT2*$^{-/-}$ *LDLr*$^{-/-}$ mice. LCAT deficiency led to an ~30% depletion of CE in the core of the LDL, with a concomitant increase in the PL on the surface of the lipoproteins. Deficiency of both LCAT and ACAT2 led to a complete absence of core CE and a significant enrichment of surface lipids (FC and PL).

Quantification of apoB accumulation rates in mouse liver perfusions demonstrated that animals deficient in ACAT2 did not decrease the mass of apoB secreted into the perfusate. In an earlier study, we determined that the

TABLE 5. Composition of LDL (1.019 < d < 1.063) isolated from plasma of knockout mice fed a 0.02% cholesterol diet

Genotype	Percentage of Total LDL Mass				
	FC	CE	TG	PL	Protein
LDLr$^{-/-}$ (n = 3)	9.4 (1.1)[a]	54.6 (1.9)[a]	5.0 (2.3)[a]	11.2 (0.9)[a]	19.9 (0.6)[a]
ACAT2$^{-/-}$ *LDLr*$^{-/-}$ (n = 5)	9.9 (1.1)[a]	51.3 (2.2)[a]	5.1 (0.8)[a]	12.7 (1.3)[a]	21.2 (0.5)[a]
LCAT$^{-/-}$ *LDLr*$^{-/-}$ (n = 3)	16.0 (3.1)[a]	38.6 (4.0)[b]	9.0 (0.8)[a,b]	19.3 (0.1)[b]	17.0 (0.7)[b]
ACAT2$^{-/-}$ *LCAT*$^{-/-}$ *LDLR*$^{-/-}$ (n = 6)	46.9 (2.9)[b]	0 (2.0)[c]	11.8 (1.5)[b]	26.7 (1.3)[b]	14.6 (0.9)[c]

LDL isolation and lipid and protein content were quantified as described in Materials and Methods. Values were calculated as percentages of the total mass of the LDL. Values represent means and (SEM). Values with different letters in the same column have statistically significant differences ($P < 0.05$); values with the same letter are not different.

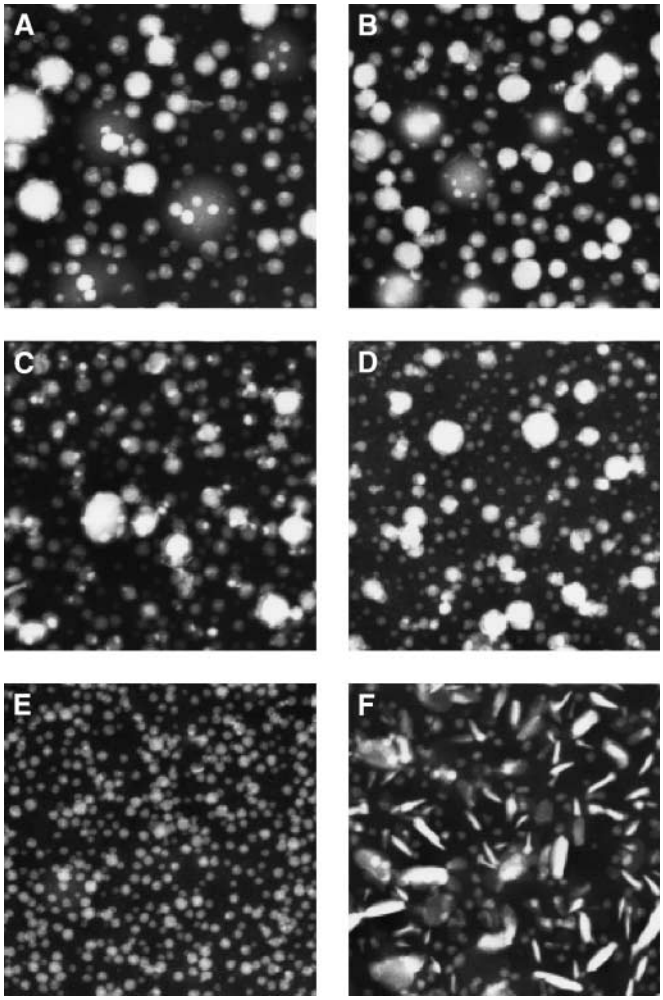

Fig. 4. Negative stain electron microscopy of apoB-containing lipoproteins isolated from liver perfusion and plasma of knockout mice fed a 0.02% cholesterol diet. Negative stain electron microscopy was carried out as described in Materials and Methods. All images are shown at a magnification of 90,000×. A: VLDL isolated from *ACAT2*$^{-/-}$ *LDLr*$^{-/-}$ mouse liver perfusion. B: VLDL isolated from *ACAT2*$^{-/-}$ *LCAT*$^{-/-}$ *LDLr*$^{-/-}$ mouse liver perfusion. C: VLDL isolated from *ACAT2*$^{-/-}$ *LDLr*$^{-/-}$ mouse plasma. D: VLDL isolated from *ACAT2*$^{-/-}$ *LCAT*$^{-/-}$ *LDLr*$^{-/-}$ mouse plasma. E: LDL isolated from *ACAT2*$^{-/-}$ *LDLr*$^{-/-}$ mouse plasma. F: LDL isolated from *ACAT2*$^{-/-}$ *LCAT*$^{-/-}$ *LDLr*$^{-/-}$ mouse plasma.

livers of *ACAT2*$^{-/-}$ *LDLr*$^{-/-}$ mice were depleted in CE content (3). This led us to conclude that in the mouse model, liver CE availability does not appear to play a regulatory role in hepatic apoB secretion.

The analysis of perfusate and plasma VLDL composition suggested that the ACAT2-dependent decreases in CE concentration of perfusate were attributable to the depletion of CE in the core of VLDLs. Although it did not reach statistical significance, we found that TG secretion into the perfusate of the *ACAT2*$^{-/-}$ *LDLr*$^{-/-}$ mice appeared to be higher. Similarly, the core of the VLDLs isolated from perfusate tended to be enriched in TG. The tendency for TG enrichment in the core of VLDL reached statistical significance in the plasma VLDL of the *ACAT2*$^{-/-}$ mice. By enriching the core in TG, the VLDL maintained the ratio of 70% of mass in the core as TG and CE and 30% on the surface as FC, PL, and protein. By conserving the percentage surface-percentage core ratio, the VLDLs of the *ACAT2*$^{-/-}$ mice maintained a spherical appearance when viewed with the electron microscope. The possibility that the protection of the surface-core ratio is vital for VLDL secretion may explain the enrichment of TG in *ACAT2*$^{-/-}$ VLDLs. In turn, this TG enrichment of VLDLs could explain the increased plasma TG levels of *ACAT2*$^{-/-}$ deficient mice (20, 21). This suggests that ACAT2 may play important roles in both cholesterol and TG metabolism.

The deficiency of LCAT and/or ACAT2 also had effects on the LDL composition of the mice. Despite the fact that VLDL in the *ACAT2*$^{-/-}$ *LDLr*$^{-/-}$ mice was depleted in CE, the CE contribution to LDL was no different in *ACAT2*$^{-/-}$ *LDLr*$^{-/-}$ mice compared with *LDLr*$^{-/-}$ controls. However, when both ACAT2 and LCAT were absent, no CE was present in the LDLs. This led us to conclude that normally, ACAT2 synthesizes VLDL CE, which, via remodeling in the plasma, becomes LDL CE. However, in the absence of ACAT2, LCAT is able to maintain the structure of the LDL by synthesizing CE. Despite the similar LDL compositions and LDL cholesterol concentrations in the *ACAT2*$^{-/-}$ *LDLr*$^{-/-}$ mice compared with *LDLr*$^{-/-}$ mice, atherosclerosis in the *ACAT2*$^{-/-}$ *LDLr*$^{-/-}$ animals was decreased by more than 90% compared with *LDLr*$^{-/-}$ controls (3). This observation implies that LCAT-derived CEs, which are enriched in polyunsaturated fatty acids (12), are less atherogenic than ACAT2-derived CEs, which are enriched in saturated and monounsaturated fatty acids. This may at least partially explain the numerous studies showing the beneficial effects on atherosclerosis of polyunsaturated fat-enriched diets compared with saturated or monounsaturated fat-enriched diets (4). These results also imply that any antiatherogenic effects of the pharmaceutical inhibition of ACAT2, for example, might be attributed to more than the lowering of LDL cholesterol concentrations.

LCAT deficiency led to significant decreases in LDL core CE and a significant increase in LDL PL, with a concomitant tendency for LDL FC to also increase. Glomset and colleagues (22) demonstrated similar results in *LCAT*$^{-/-}$ patients, leading them to conclude that the phospholipase activity of LCAT is essential in the removal of excess surface lipid during the lipolytic conversion of VLDL to LDL. Our results expand on this conclusion in that LCAT also contributes CE to the core of LDL, particularly in the face of ACAT2 deficiency. Deficiency of both LCAT and ACAT2 had dramatic effects on the composition and morphology of the LDLs. Although ~60% of the mass of the LDL was located in the core and 40% on the surface in *LDLr*$^{-/-}$ mice, almost 90% of the LDL mass was located on the surface of the LDLs of the *ACAT2*$^{-/-}$ *LCAT*$^{-/-}$ *LDLr*$^{-/-}$ mice. This enrichment in surface lipid and depletion in core lipids led to the LDLs taking on a disc-shaped or flattened appearance when observed by electron microscopy. These discoidal structures have a relatively large diameter that clarifies the observation that all apoB-containing lipoproteins in this mouse genotype elute in the VLDL size fraction when separated by size on HPLC (3).

Furthermore, the observations here with liver perfusion show that the unusual LDL structures are not a hepatic secretion product. Evidently, these lipoproteins are not atherogenic, as previous results indicate that *ACAT2*$^{-/-}$ *LCAT*$^{-/-}$ *LDLr*$^{-/-}$ mice have no signs of aortic atherosclerosis when fed a 0.1% cholesterol diet for 20 weeks (3). It is possible that, because of this abnormal morphology, these lipoproteins are unable to easily penetrate the endothelial cells of the vessel wall and, therefore, the FC contained on the lipoproteins does not accumulate in the artery.

In summary, these studies show that hepatic ACAT2 is essential for the incorporation of CE into the core of VLDLs, but they do not show a role for the enzyme in the regulation of the number of apoB-containing lipoproteins secreted. With respect to the LDL fraction, it was found that LCAT is important in removing excess surface lipid generated from the lipolysis of TG in the core of VLDLs and is able to compensate for the loss of hepatic ACAT2 by synthesizing CE on the lipoproteins. Despite these compensatory mechanisms, previous studies show that atherosclerosis was decreased by 90%, suggesting that the incorporation of LCAT-derived CE into LDLs was less atherogenic than the incorporation of ACAT2-derived CE. Therefore, this study is also consistent with the suggestion that the primary antiatherosclerotic effects of ACAT2 inhibition are not associated with the lowering of LDL cholesterol levels.

This work was made possible with the support of the National Institutes of Health, including National Heart, Lung, and Blood Institute Grants HL-49373, HL-24736, and HL-054176. R.G.L. was supported by National Institutes of Health Training Grants HL-07668 and HL-07115-28. This work represents a portion of that completed by R.G.L. for the Ph.D. degree at Wake Forest University Graduate School of Arts and Sciences.

REFERENCES

1. Kannel, W. B., W. P. Castelli, T. Gordon, and P. M. McNamara. 1971. Serum cholesterol, lipoproteins, and the risk of coronary heart disease. The Framingham Study. *Ann. Intern. Med.* **74:** 1–12.
2. Merkel, M., W. Velez-Carrasco, L. C. Hudgins, and J. L. Breslow. 2001. Compared with saturated fatty acids, dietary monounsaturated fatty acids and carbohydrates increase atherosclerosis and VLDL cholesterol levels in LDL receptor-deficient, but not apolipoprotein E-deficient, mice. *Proc. Natl. Acad. Sci. USA.* **98:** 13294–13299.
3. Lee, R. G., K. L. Kelley, J. K. Sawyer, R. V. Farese, Jr., J. S. Parks, and L. L. Rudel. 2004. Plasma cholesteryl esters provided by lecithin: cholesterol acyltransferase and acyl-coenzyme A:cholesterol acyltransferase 2 have opposite atherosclerotic potential. *Circ. Res.* **95:** 998–1004.
4. Lada, A. T., and L. L. Rudel. 2003. Dietary monounsaturated versus polyunsaturated fatty acids: which is really better for protection from coronary artery disease? *Curr. Opin. Lipidol.* **14:** 41–46.
5. Schrade, W., E. Boehle, M. D. Frankfurt, and R. Biegler. 1960. Humoral changes in arteriosclerosis. Investigations of lipids, fatty acids, ketone bodies, pyruvic acid, lactic acid, and glucose in the blood. *Lancet.* **ii:** 1409–1416.
6. Lawrie, T. D. V., S. G. McAlpine, B. M. Rifkind, and J. F. Robinson. 1961. Serum fatty-acid patterns in coronary-artery disease. *Lancet.* **i:** 421–424.
7. Kirkeby, K., P. Ingvaldsen, and I. Bjerkedal. 1972. Fatty acid composition of serum lipids in men with myocardial infarction. *Acta Med. Scand.* **192:** 513–519.
8. Kingsbury, K. J., C. Brett, R. Stovold, A. Chapman, J. Anderson, and D. M. Morgan. 1974. Abnormal fatty acid composition and human atherosclerosis. *Postgrad. Med. J.* **50:** 425–440.
9. Rudel, L. L., J. S. Parks, and J. K. Sawyer. 1995. Compared with dietary monounsaturated and saturated fat, polyunsaturated fat protects African green monkeys from coronary artery atherosclerosis. *Arterioscler. Thromb. Vasc. Biol.* **15:** 2101–2110.
10. Rudel, L. L., J. Haines, J. K. Sawyer, R. Shah, M. S. Wilson, and T. P. Carr. 1997. Hepatic origin of cholesteryl oleate in coronary artery atherosclerosis in African green monkeys. Enrichment by dietary monounsaturated fat. *J. Clin. Invest.* **100:** 74–83.
11. Furbee, J. W., Jr., J. K. Sawyer, and J. S. Parks. 2002. Lecithin:cholesterol acyltransferase deficiency increases atherosclerosis in the low density lipoprotein receptor and apolipoprotein E knockout mice. *J. Biol. Chem.* **277:** 3511–3519.
12. Furbee, J. W., Jr., O. Francone, and J. S. Parks. 2002. In vivo contribution of LCAT to apolipoprotein B lipoprotein cholesteryl esters in LDL receptor and apolipoprotein E knockout mice. *J. Lipid Res.* **43:** 428–437.
13. Rudel, L. L., K. Kelley, J. K. Sawyer, R. Shah, and M. D. Wilson. 1998. Dietary monounsaturated fatty acids promote aortic atherosclerosis in LDL receptor-null, human apoB100-overexpressing transgenic mice. *Arterioscler. Thromb. Vasc. Biol.* **18:** 1818–1827.
14. Johnson, F. L., R. W. St. Clair, and L. L. Rudel. 1983. Studies of the production of low density lipoproteins by perfused livers from nonhuman primates: effect of dietary cholesterol. *J. Clin. Invest.* **72:** 221–236.
15. Bligh, E. G., and W. J. Dyer. 1959. A rapid method of total lipid extraction and purification. *Can. J. Biochem. Physiol.* **37:** 911–917.
16. Carr, T. P., C. J. Andresen, and L. L. Rudel. 1993. Enzymatic determination of triglyceride, free cholesterol, and total cholesterol in tissue lipid extracts. *Clin. Biochem.* **26:** 39–42.
17. Fiske, C. A., and Y. SubbaRow. 1925. The colorimetric determination of phosphorus. *J. Biol. Chem.* **66:** 375–400.
18. Lowry, O. J., N. J. Rosebrough, A. L. Farr, and R. J. Randall. 1951. Protein measurement with the Folin phenol reagent. *J. Biol. Chem.* **19:** 265–275.
19. Hamilton, R. L., Jr., J. Goerke, L. S. S. Guo, M. C. Williams, and R. J. Havel. 1980. Unilamellar liposomes made with the French pressure cell: a simple preparative and semiquantitative technique. *J. Lipid Res.* **21:** 981–992.
20. Buhman, K. K., M. Accad, S. Novak, R. S. Choi, J. S. Wong, R. L. Hamilton, S. Turley, and R. V. Farese, Jr. 2000. Resistance to diet-induced hypercholesterolemia and gallstone formation in ACAT2-deficient mice. *Nat. Med.* **6:** 1341–1347.
21. Willner, E. L., B. Tow, K. K. Buhman, M. Wilson, D. A. Sanan, L. L. Rudel, and R. V. Farese. 2003. Deficiency of acyl CoA:cholesterol acyltransferase 2 prevents atherosclerosis in apolipoprotein E-deficient mice. *Proc. Natl. Acad. Sci. USA.* **100:** 1262–1267.
22. Forte, T., K. R. Norum, J. A. Glomset, and A. V. Nichols. 1971. Plasma lipoproteins in familial lecithin:cholesterol acyltransferase deficiency: structure of low and high density lipoproteins as revealed by electron microscopy. *J. Clin. Invest.* **50:** 1141–1148.